

## Two-Dimensional Miscibility Studies—The Analysis of Interaction between Long-Chain Alcohols and Semifluorinated Alkanes

Marcin Broniatowski,<sup>†</sup> Nuria Vila Romeu,<sup>‡</sup> and Patrycja Dynarowicz-Łątka<sup>\*,†</sup>

Department of General Chemistry, Faculty of Chemistry, Jagiellonian University, Ingardena 3, 30–060 Kraków, Poland, and Department of Physical Chemistry, Faculty of Sciences, University of Vigo, Campus As Lagoas s/n 32004 Ourense, Spain

Received: October 19, 2005; In Final Form: January 3, 2006

This work presents the results of phase behavior studies of two-dimensional (2D) binary systems involving semifluorinated alkanes (SFAs) and fatty alcohols. Four different SFAs were selected for investigations: (i) with a short and branched perfluorinated moiety (iF3H20), (ii) with a short and normal perfluorinated chain (F4H20), (iii) with a long and branched perfluorinated fragment (iF9H20), and (iv) with a long and normal perfluorinated group (F10H20). Two alcohols were selected to mix with the above-mentioned SFAs: tetradecanol and docosanol. The measurements were based on surface pressure/area isotherms in addition to Brewster angle microscope (BAM) imaging. Dependencies of the collapse surface pressure and the compression modulus vs the monolayer composition together with the excess free energy of mixing values, complemented with BAM images, enabled us to draw some general conclusions regarding the phase behavior of the investigated mixed systems. Generally, it has been noticed that the addition of docosanol into an SFA monolayer exerts a condensing effect, contrary to tetradecanol. Moreover, SFAs with a long perfluorinated segment mix to a larger extent with alcohols as compared to their analogues having a short perfluorinated moiety. The resultant phase diagrams for all the investigated eight mixtures are presented and discussed.

### 1. Introduction

Amphiphilic molecules built of two opposing parts, hydrophilic and hydrophobic, which are covalently bound together, are crucial for all living organisms. The functions of a living cell would not be possible without different kinds of lipids, steroids, fatty acids, and many other molecules having amphiphilic character. Investigation of the properties of such molecules of biological importance was the main driving force for the development of surface chemistry.<sup>1</sup> Of course, amphiphiles of biomedical importance do not function in cell membranes or other organelles alone in isolated clusters, but they interact with many other substances, like proteins or other amphiphiles. The need of a better understanding of the constitution and function of such organelles leads to the investigation of mixed films: binary, ternary, or—rarely—having more than three components. Mixed films often show pronouncedly different interfacial properties as compared to their individual components. Investigations of two-dimensional (2D) mixtures are vital in the development of new medicines, and very often, research studies on molecular models are carried out before testing a new drug on living cells or animals, since these kinds of studies are significantly less expensive, are easier to perform, and provide a plethora of important results. Dipalmitoylphosphocholine (DPPC)<sup>2</sup>—a well-known model lung surfactant—is always administered with cosurfactants, like hexadecanol and tyloxapol<sup>3</sup> and, therefore, has been investigated in many different kinds of mixed films, for example, in mixtures with long-chained alcohols<sup>4</sup> or cholesterol.<sup>5,6</sup> The antibacterial or antifungal activity

of many antibiotics is strongly related to their interaction with bacterial or fungal cell membrane components, and therefore, a great number of monolayer studies of binary or ternary systems containing an antibiotic molecule and a cell membrane component have been carried out, e.g., mixtures of valinomycin with cholesterol and stearic acid,<sup>7</sup> bacteriocin and a phospholipid,<sup>8</sup> amphotericin B and different sterols<sup>9</sup>, or gramicidin A and ethyl palmitate.<sup>10</sup> Other research projects involve studies of ceramides in mixed films with cholesterol and fatty acids,<sup>11,12</sup> mixtures of modified vitamins,<sup>13</sup> or an anticancer drug—miltefosine—mixed with a model ganglioside<sup>14</sup> or membrane phospholipids.<sup>15</sup>

As far as drugs of amphiphilic character or interacting with amphiphilic molecules in cell membranes are concerned, a lot of effort has been undertaken in designing and introducing into the market fluorinated surfactants of biomedical activity.<sup>16,17</sup> The interaction of fluorocarbons and hydrocarbons in liquids and gases is highly nonideal, and pure hydrocarbons and their perfluorinated analogues are known to segregate. This issue was originally investigated by Scott<sup>18</sup> and furthered by Hildebrand,<sup>19</sup> which was of important impact in the construction of the regular solution theory. Fluorinated surfactants were thoroughly investigated by Mukerjee and co-workers in the seventies and eighties of the previous century<sup>20,21</sup> and were a subject of investigations of many other scientific groups all over the world. Studies of the interactions between the hydrogenated and perfluorinated phases, introduced by Scott and Hildebrand in bulk systems, were later adopted to the 2D systems, and a great number of binary and ternary mixtures containing fluorinated surfactants have been investigated so far, for example, perfluorinated<sup>22</sup> or partially fluorinated (semifluorinated) fatty acids<sup>23</sup> in mixtures with phospholipids, DPPC with partially fluorinated carboxylic acid,<sup>24</sup> perfluoroalkylated phospholipid with either fatty acids<sup>25</sup> or a semifluorinated alcohol,<sup>26</sup> or a native phospholipid.<sup>27</sup> The

\* Corresponding author. Tel.: +48-12-6632082. Fax: +48-12-6340515. E-mail: ucdynaro@cyf-kr.edu.pl.

<sup>†</sup> Jagiellonian University.

<sup>‡</sup> University of Vigo, Campus As Lagoas.

extent to which fluorocarbon and hydrocarbon amphiphiles are miscible depends on their chemical structure; in general, the stronger the headgroup–headgroup interactions, the better mutual miscibility of a fluorinated and hydrogenated amphiphile in a mixed film is observed.<sup>24</sup> It is of great interest to investigate the tail–tail interactions in binary system containing fluorinated and hydrogenated surfactants. To reach this goal, the headgroup of the investigated amphiphile should be simplified and lessened to limit possible interference from the head–head interaction. The work of Shibata and co-workers, where the properties of mixed binary films formed by tetradecanoic acid and perfluorocarboxylic acids differing in the length of the perfluorinated chain were studied,<sup>28</sup> can serve as an example of such projects. The most appropriate molecules for investigations aiming at researching tail–tail interactions are compounds lacking a headgroup in their structure. Normal long-chained alkanes cannot be applied for this purpose, since they do not spread at the air/water interface but form multilayer lenses.<sup>1</sup> On the contrary, semifluorinated alkanes, which also do not have any polar group, seem to be very useful in these kinds of studies as they are known to be surface active<sup>29</sup> and are capable of Langmuir monolayer formation.<sup>30,31</sup>

Semifluorinated alkanes (SFAs) are diblock molecules, of the general formula  $F(CF_2)_m(CH_2)_nH$  ( $FmHn$ ), in which perfluorinated and hydrogenated moieties are covalently bound. At the air/water interface, SFAs form highly organized and stable monolayers and are oriented with their perfluorinated part toward air, while their hydrogenated fragment remains in contact with water.<sup>32,33</sup> Although a great deal of information about Langmuir monolayers formed by different SFAs has already been reported, very little is known about the behavior of semifluorinated alkanes in 2D mixtures. Some preliminary results have appeared in recent years regarding surface mixtures of F8H16 with phospholipids<sup>34,35</sup> or diunsaturated polymerisable fatty acid<sup>36</sup> and F8H18 with poly(ethylene oxide) diblock copolymer.<sup>37</sup> In all these studies, the hydrogenated component of the binary 2D mixtures had a large and complicated headgroup<sup>34,35,37</sup> or possessed unsaturated bonds (two alkynes triple bonds) in the hydrogenated chain.<sup>36</sup>

The aim of the present paper was the investigation of binary mixtures containing different SFAs and hydrogenated amphiphiles with one normal saturated hydrogenated chain and the headgroup as small and as simple as possible. It is evident that such criteria are entirely fulfilled by long-chained normal alcohols. The hydroxyl group seems to be the smallest possible polar group, and because it is not ionizable, it is easy to investigate because no control of the water subphase pH is necessary, contrary to the case of other amphiphilic molecules, such as, for example, carboxylic acids. Information on the chain–chain interactions and chain lengths exerting the most favorable effects can be valuable in the design of new detergents or lubricants. Mixtures of semifluorinated alkanes/normal alcohols can be treated as model systems, and the obtained results can be of importance in researching more complicated systems containing SFAs, such as, for example, mixtures with different phospholipids, steroids, triglycerides, or gangliosides.

For this investigation, we have chosen four different SFAs: all of them can be considered as  $\omega$ -perfluoroalkylated derivatives of eicosane. All of them have 20 carbon atoms in the hydrogenated moiety, but they differ in the length and structure of their perfluorinated fragments. Two of them have a short perfluorinated moiety, perfluoroisopropyl and perfluorobutyl (iF3H20  $M = 450.6$  g/mol; F4H20  $M = 500.6$  g/mol, respectively), while two others have long perfluorinated group,

perfluoroisononyl and perfluorodecyl (iF9H20  $M = 750.6$  g/mol; F10H20  $M = 800.6$  g/mol, respectively). Two compounds investigated here have *iso*-branching at their perfluorinated end, whereas two others have their perfluorinated moiety in an unbranched (normal) arrangement. Such a choice of semifluorinated alkanes enables us to study the influence of the length and structure of the perfluorinated segment on the behavior of SFAs in binary 2D films at the air/water interface. As far as the alcohols are concerned, we have selected *n*-tetradecanol (C14OH) and *n*-docosanol (C22OH), which differ by eight methylene groups in the length of the hydrocarbon tail. We have also done preliminary experiments employing longer alcohols, namely tetracosanol (C24OH) and triacontanol (C30OH); however, the obtained results were very similar to those recorded for C22OH and, therefore, are not presented here. It is worthy pointing out that such long alkyl chains such as C24/C30 are of less biomedical interest since they are normally not found in living organisms. Another factor affecting our choice, as regards alcohol molecules, was the characteristics of monolayers formed by the selected two alcohols: namely, monolayers of docosanol are of the condensed, solid type, while monolayers of tetradecanol are more expanded and have liquid-condensed character<sup>1</sup>. In our research, we have applied classical methods as surface manometry (surface pressure–area isotherms) as well as modern methods of monolayer characterization, such as Brewster angle microscopy (BAM).

## 2. Experimental Section

The investigated semifluorinated alkanes were synthesized by one of us (M.B.), following the procedure of Rabolt et al.,<sup>38</sup> which is based on a radical addition of a perfluoroalkyl iodide to a respective alkene, initiated by AIBN, followed by reductive detachment of the iodine atom. Syntheses of F10H20 and F4H20 are described elsewhere,<sup>32,33</sup> while *iso*-branched SFAs were not synthesized before. The following substrates, perfluoroisopropyl iodide and perfluoroisononyl iodide (>98%), were purchased from Fluorochem, while eicosene (98%) was supplied by Fluka. The purities of iF3H20 and iF9H20 were verified by elemental analysis: iF3H20 theoretically: C, 61.31; H, 9.17. Found C, 61.25; H, 9.09. iF9H20 theoretically: C, 46.40; H, 5.50. Found: C, 46.51; H, 5.44. The purity of these two compounds was also corroborated by <sup>1</sup>H and <sup>13</sup>C NMR, mass spectroscopy, and differential scanning calorimetry. 1-Tetradecanol (99%, C<sub>14</sub>H<sub>29</sub>OH, (C14OH)) and 1-docosanol (99%, C<sub>22</sub>H<sub>45</sub>OH, (C22OH)) were purchased from Fluka and used as received.

The spreading solutions for the monolayer experiments were prepared by dissolving each compound in chloroform (Aldrich, HPLC grade) with a typical concentration of ca. 0.5 mg/mL. Mixed solutions were prepared from the respective stock solutions of both compounds. The number of molecules spread on the water subphase ( $7.5 \times 10^{16}$  molecules), with a Hamilton microsyringe, precise to  $\pm 0.2$   $\mu$ L, was kept constant in all experiments. Ultrapure water (produced by a Nanopure coupled to a Milli-Q water purification system (resistivity = 18.2 M $\Omega$  cm) was used as a subphase. The subphase temperature was 20 °C and was controlled to within 0.1 °C by a circulating water system from Haake. Experiments were carried with a NIMA 601 trough (Coventry, U.K.) (total area = 600 cm<sup>2</sup>, equipped with two symmetrical barriers) and placed on an antivibration table. Surface pressure was measured with the accuracy of  $\pm 0.1$  mN/m using a Wilhelmy plate made from chromatography paper (Wharman Chr1) as a pressure sensor. After spreading, the monolayers were left for 10 min to ensure solvent evaporation, after which the compression was initiated with a barrier speed

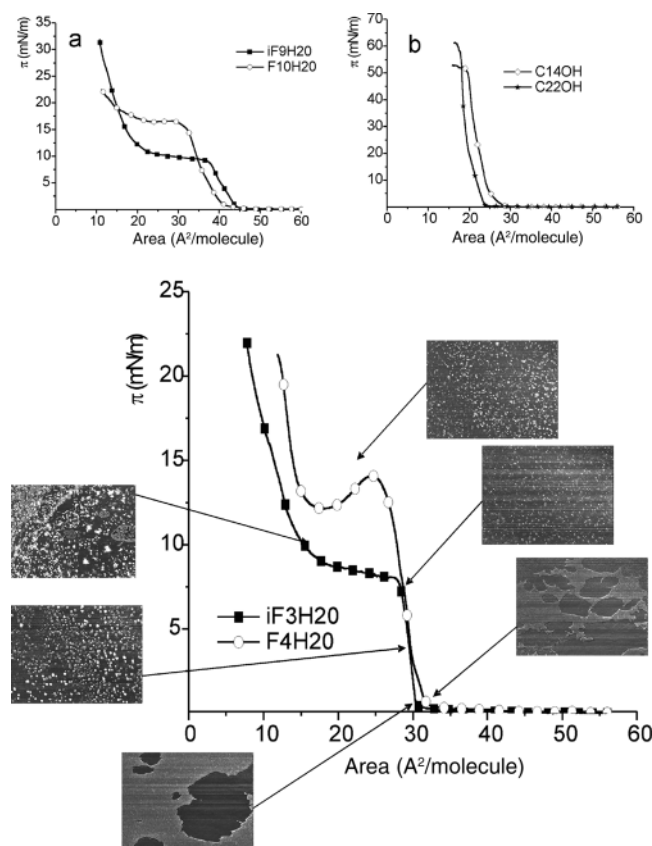


**Figure 1.** Plots of  $\pi$ - $A$  isotherms of iF3H20 and F4H20 together with BAM images and  $\pi$ - $A$  isotherms for iF9H20 and F10H20 (inset a) and for C14OH and C22OH (inset b).

of 15 cm<sup>2</sup>/min. A Brewster angle microscope BAM 2 plus (NFT, Germany) was used for microscopic observation of the monolayers structure. It is equipped with a 50 mW laser, emitting *p*-polarized light of 532 nm in wavelength, that was reflected off the air/water interface at approximately 53.1° (the Brewster angle). The lateral resolution of the microscope was 2  $\mu$ m. The images were digitized and processed to obtain the best quality of the BAM pictures. Each image corresponds to a 228  $\mu$ m  $\times$  170  $\mu$ m area of the monolayer's fragment.

### 3. Results

To begin with, a brief description of the monolayer characteristics of pure compounds will be provided. Figure 1 shows the  $\pi$ - $A$  isotherms for iF3H20 and iF4H20 together with BAM images registered at different surface pressure regions, while the insets present the isotherms for iF9H20 and F10H20 as well as for C14OH and C22OH (insets a and b, respectively). Surface pressure starts to rise at about 35 A<sup>2</sup>/molecule for SFAs with a short perfluorinated fragment versus 45 A<sup>2</sup>/molecule for compounds with a longer perfluorinated chain. After a region of steep increase of the surface pressure, film collapse occurs. It is worth noticing that SFAs with *iso*-branching in their perfluorinated part have a lower collapse pressures as compared to those possessing a normal perfluorinated chain: ca. 8 vs ca. 15 mN/m, respectively. As far as the BAM textures of the pure compounds are concerned, long-chain alcohols and SFAs with a long perfluorinated moiety form homogeneous Langmuir monolayers, i.e., no structures are visible upon compression until the collapse is reached. Only at the beginning of compression, at large molecular areas corresponding to the equilibrium between gaseous and liquid expanded states of the monolayer, some foamlike structures can be observed. BAM textures of

SFAs with a long perfluorinated moiety were already discussed in our previous contribution.<sup>32</sup> Since the architecture of the iF9H20 monolayer was found to be quite similar to that observed for F10H20, the images were not presented herein. The situation for SFAs with a short perfluorinated fragment is slightly different, and some representative BAM images for iF3H20 and F4H20 are included in Figure 1. Similarly to SFAs with a long perfluorinated chain, iF3H20 and F4H20 form foamlike structures at low surface pressures, typical for gaseous/liquid expanded equilibrium; however, upon further compression before the collapse, unlike F10H20 and iF9H20, white spots are already visible in the BAM images, the number of which increases with rising surface pressure. These white spots can be interpreted as nuclei of a new three-dimensional (3D) phase. This indicates that monolayers of iF3H20 and F4H20 are less stable than those formed by SFAs with a longer perfluorinated moiety.

While describing the characteristics of pure SFA and alcohol monolayers, it is useful to remark on the models of monolayer collapse, because profound differences in the collapse process can be observed for SFAs with a long perfluorinated moiety and alcohols used in or study versus SFAs with a short perfluorinated fragment. Generally, two different mechanisms of monolayer collapse have been described in the literature. One of them is the mechanism of monolayer folding: according to Ries and Kinball,<sup>39</sup> before the final stage of collapse is reached, some folds in a monolayer start to appear, leading—upon further compression—to film collapse, which is understood in this approach as the formation of three-layer regions. Such folds were observed with fluorescence and BAM microscopy<sup>40</sup> for lung surfactants. According to the other model, monolayer collapse is due to the formation of 3D crystallites at the air/water interface upon film compression. These crystallites are present already at the precollapse region, and upon reaching the collapse pressure, the growth of the crystallites leads to the fall of surface pressure or to the appearance of a flat plateau on the course of the  $\pi$ - $A$  isotherms.<sup>41</sup> Monolayers from surfactants forming stable Langmuir monolayers, like long-chain normal alcohols and—in our opinion—also SFAs with a long perfluorinated and hydrogenated moiety (as in F10H20), collapse according to the folding model. In BAM images, their monolayers are usually structureless and homogeneous upon compression; however, upon reaching the collapse, bright strips and large white flocks of the collapsed material are clearly visible. On the contrary, monolayers from compounds forming less stable monolayers, often having low values of collapse pressure, are reported to collapse according to the second mechanism. Their BAM images show white spots corresponding to the 3D crystallites, visible already in the precollapse region. At the collapse, the image is very similar, only the number of white spots is larger. It seems that iF3H20 and F4H20 collapse according to this very mechanism.

Moreover, bulk melting temperatures of semifluorinated alkanes can be of help in understanding their monolayer properties. The compounds with a short perfluorinated fragment, i.e., F4H20 and iF3H20, melt at 31.3 °C and 29.8 °C, respectively, while molecules with a long perfluorinated moiety used in this study, i.e., F10H20 and iF9H20, melt at 76.5 °C and 51.2 °C, respectively. Samples of all the investigated SFAs were investigated using differential scanning calorimetry (DSC) performed at different cooling/heating modes. This method also proved a high purity of the studied compounds (a very narrow melting peak in the DSC curve). Generally, chemicals of lower melting temperature form less stable and more expanded



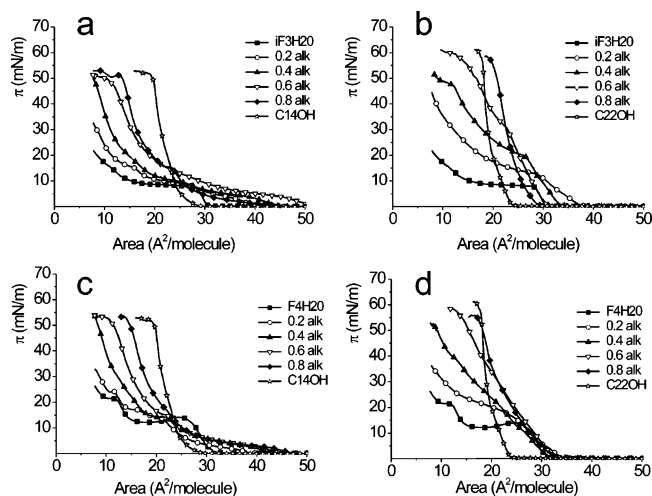


**Figure 2.** Plots of  $\pi$ – $A$  isotherms for the mixed monolayers formed by iF3H20 and F4H20: (a) iF3H20/C14OH; (b) iF3H20/C22OH; (c) F4H20/C14OH; (d) F4H20/C22OH.

monolayers than similar molecules possessing higher melting points<sup>39</sup>. However, it is worth mentioning that all monolayer experiments in this study were carried out at 20 °C, where all the studied SFAs are in the solid state.

The  $\pi$ – $A$  isotherms registered for tetradecanol and docosanol (inset Figure 1b) are in a good agreement with literature data.<sup>1,42,43</sup> In fact, long-chained alcohols are often taken as model surfactants. When comparing the isotherms for both investigated alcohols, it can be noticed that C14OH forms more expanded monolayers than C22OH. This fact is of importance in further discussion of the properties of mixed films formed by the investigated alcohols and SFAs.

**3.1 Mixed Monolayers Formed by SFAs with a Short Perfluorinated Moiety.** In the first step, the results obtained for mixed monolayers of an SFA with a short perfluorinated chain (iF3H20 and F4H20) and C14OH/C22OH will be presented. In our experiments, the mole fraction of a given alcohol was changed with the interval of 0.1, starting from a pure SFA monolayer (0 mol fraction of alcohol) and ending on a pure alcohol monolayer ( $X(\text{alcohol}) = 1$ ). Figure 2 shows isotherms for the mixtures of iF3H20 and C14OH (Figure 2a), iF3H20 and C22OH (Figure 2b), F4H20 and C14OH (Figure 2c), and F4H20 and C22OH (Figure 2d). For clarity of presentation, only isotherms for mixed monolayers with the interval of  $X(\text{alcohol}) = 0.2$  are shown in the figure.

There is a general difference visible between mixed monolayers containing C14OH and C22OH. Isotherms recorded for different compositions of iF3H20 and C14OH or F4H20 and C14OH are more expanded than the isotherms of individual components (at surface pressures lower than the collapse pressure of a pure SFA monolayer). This means that mixed film molecules are less ordered as compared to one-component monolayers. In contrast, the addition of C22OH to the monolayers of either iF3H20 or F4H20 has a condensing effect, since the isotherms of mixed monolayers are mainly situated between the isotherm of pure SFA and C22OH. According to the phase rule,<sup>44</sup> the collapse pressure ( $\pi_c$ ) for a 2D binary system is a good indicator of mutual miscibility. For immiscible systems, the collapse pressure does not depend on the proportion of the components, and two separate collapse pressures, characteristic of each component, are observed, whereas in a miscible system the  $\pi_c$  value changes from the value characteristic of one component to the value characteristic of the other one upon increasing the mole fraction of the second component. In the

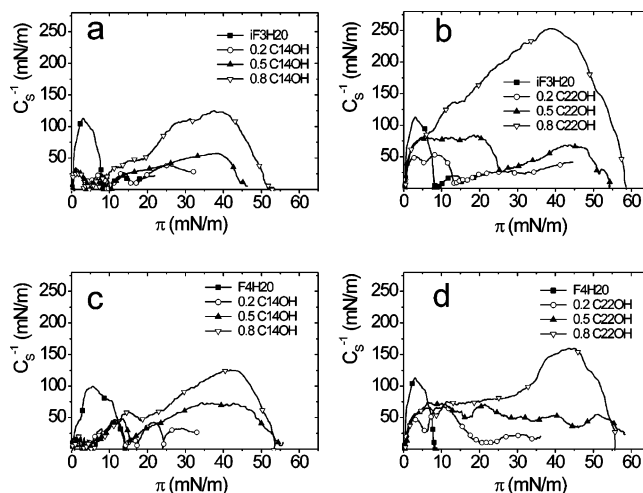


**Figure 3.**  $C_s^{-1}$ – $\pi$  dependences for the systems containing iF3H20 and F4H20: (a) iF3H20/C14OH; (b) iF3H20/C22OH; (c) F4H20/C14OH; (d) F4H20/C22OH.

case of the 2D binary systems investigated in this work, the problem arises with a precise determination of the collapse pressure values directly for the  $\pi$ – $A$  isotherms (Figure 2).

A tool, which can be of help in solving this problem and can be used to identify the state of the investigated monolayers, is the compression modulus,  $C_s^{-1}$ , defined as  $-A(d\pi/dA)$ .<sup>42,43</sup> Values of  $C_s^{-1}$  lower than 12.5 mN/m indicate a gaseous monolayer state; from 12.5 to 100 mN/m, a liquid expanded state; from 100 to 250 mN/m, a liquid condensed state, while those greater than 250 are characteristic of the solid state of a Langmuir monolayer. At the collapse pressure,  $C_s^{-1} = 0$ , and the precise determination of  $\pi_c$  is therefore very easy from the  $C_s^{-1}$  vs  $\pi$  plots.

The plots of  $C_s^{-1}$  vs  $\pi$  for the investigated systems containing an SFA with a short perfluorinated moiety are presented in Figure 3. For clarity of presentation, only dependencies for an alcohol mole fraction equal to 0.2, 0.5, and 0.8 are shown in this figure. In the compression modulus–surface pressure plots for iF3H20/C14OH (Figure 3a), two different regions are visible, i.e., corresponding to that for pure SFA and that characteristic of tetradecanol. At low proportions of C14OH, the mixed monolayer containing iF3H20 collapses at ca. 8 mN/m, whereas, at mole fractions of C14OH greater than 0.5, iF3H20 is expelled from the alcohol monolayer at ca. 5 mN/m. Thus, it may be supposed that the two compounds are not miscible at any mixed film composition. A similar situation can be observed for F4H20/C14OH (Figure 3c) as two separate collapses can be noticed; however, contrary to the system of iF3H20/C14OH, no changes to the first collapse pressure upon increasing alcohol content were observed. The  $C_s^{-1}$ – $\pi$  plots for mixtures containing C22OH (Figure 3b and d) are different since  $\pi_c$  values obtained from the  $C_s^{-1}$ – $\pi$  curves are found to depend on the proportion of the alcohol and semifluorinated alkane.

Figure 4 presents the plots of  $\pi_c$  vs alcohol mole fraction for the systems containing SFAs with a short perfluorinated moiety. It is clearly visible that for mixtures containing C14OH in a wide range of mole fractions  $\pi_c$  is nearly constant and does not depend on the mole fraction of C14OH, which can be evidence for a phase separation in these systems. Additional proof supporting the existence of a phase separation in these systems is the fact that collapse pressures of iF3H20 approach the value of ca. 5 mN/m when the mole fraction of C14OH exceeds 0.5. In contrast, for mixtures containing C22OH,  $\pi_{coll}$  depends on  $X(\text{C22OH})$  and increases with the rising alcohol

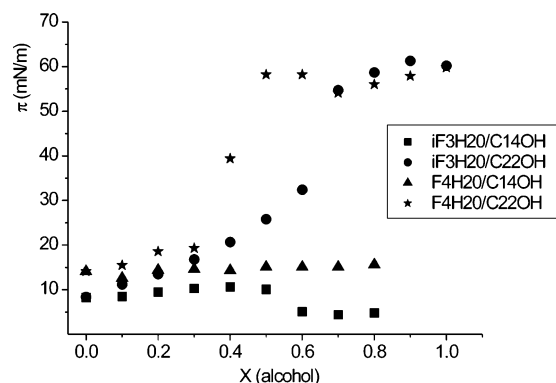


**Figure 4.** Collapse pressures ( $\pi_C$ ) vs alcohol mole fraction ( $X$ ) for the systems containing iF3H20 and F4H20.

proportion in the mixed film. This leads to the conclusion that iF3H20 or F4H20 mix with C22OH in Langmuir monolayers.

Another criterion applied for the study of binary surface films is the excess free energy of mixing ( $\Delta G^{\text{exc}}$ ) and its dependence on the composition of a mixed film at a given surface pressure value.  $\Delta G^{\text{exc}}$  is defined as follows:<sup>44</sup>

$$\Delta G^{\text{exc}} = \int_0^\pi (A_{12} - (A_1 X_1 + A_2 X_2)) d\pi \quad (1)$$

where  $A_{12}$  is the average surface area per molecule in the mixed monolayer and  $A_1$  ( $A_2$ ) stands for the molecular area of a single component monolayer at the same surface pressure as it is applied to determine  $A_{12}$  in the mixture, while  $X_1$  and  $X_2$  are the mole fractions of component 1 and 2 in the mixed film. From the values of  $\Delta G^{\text{exc}}$ , the interaction parameter ( $\alpha$ ) at different surface pressures can be calculated using the following expression:

$$\alpha = \frac{\Delta G^{\text{exc}}}{RT(X_1 X_2^2 + X_2 X_1^2)} \quad (2)$$

where  $R$  is the gas constant and  $T$  is the absolute temperature (20 °C, i.e., 293.16 K in our case). Negative values of  $\alpha$  indicate that the interactions between unlike molecules are more attractive in a binary film than in pure monolayers, while a positive sign of  $\alpha$  suggests that the interactions between unlike molecules in the mixture are repulsive or less attractive than between like molecules in their pure monolayers.

For all four systems discussed here, values of the excess energy of mixing  $\Delta G^{\text{exc}}$  were calculated for selected surface pressure values and, then, the interaction parameter  $\alpha$  was determined. As far as the values of surface pressures, for which  $\alpha$  was calculated, are concerned, we have selected several values below the collapse pressure of a pure SFA monolayer, i.e., below 8 mN/m for iF3H20 and below 14 mN/m for F4H20.

The resultant plots of  $\alpha$  vs the mole fraction of a given alcohol are presented in Figure 5. For all four cases, the  $\alpha$  values are positive, which suggests that the interactions between the alcohol and SFA molecules are less attractive than in pure one-component monolayers. The most positive values of  $\alpha$  were observed for the following mixtures, iF3H20/C14OH and F4H20/C14OH, whereas for the investigated systems containing C22OH the calculated values of  $\alpha$  were lower as compared to iF3H20/C14OH. Higher  $\alpha$  values for mixtures containing tetradecanol are in accordance with the above-presented  $C_S^{-1} - \pi$  and  $\pi_C - X(\text{alcohol})$  dependencies and, additionally, prove the existence of phase separation in these systems. Regarding mixtures with docosanol, values of  $\alpha$  are lower as compared to

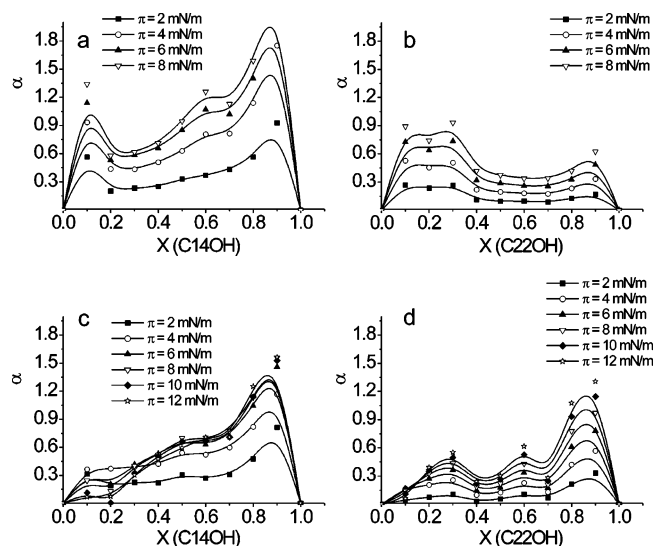


**Figure 5.** Interaction parameters ( $\alpha$ ) vs alcohol mole fraction ( $X$ ) for the systems containing iF3H20 and F4H20.

tetradecanol-containing mixtures; however, they are still positive. Although these results do not support conclusions drawn on the basis of  $\pi_C$  and  $C_S^{-1}$  vs  $X(\text{C22OH})$  dependencies, they do not exclude the possibility of the existence of a single-phase system for particular compositions of a mixed monolayer.

$C_S^{-1}$ ,  $\Delta G^{\text{exc}}$ , and  $\alpha$  have been calculated from the  $\pi - A$  datapoints, and therefore, another independent method is necessary to provide decisive proof of the phase behavior in the investigated systems. For this purpose, BAM imaging has been applied, because it enables direct visualization of the monolayer structure. Each monolayer was observed in the whole range of compression values, and a great number of BAM images was registered, from which some selected representative photos, taken at 5 mN/m for the alcohol mole fractions 0.2, 0.5, and 0.8, are presented in this paper. This particular value of  $\pi$  was chosen to visualize monolayers under similar experimental conditions. Moreover, as was mentioned above, for some proportion of C14OH, iF3H20 was found to collapse at a low value of  $\pi$ , 5 mN/m, and therefore, it was evident that at higher  $\pi$  values the phases were obviously separated. The images for systems containing iF3H20 are gathered in Figure 6, while those containing F4H20 are presented in Figure 7.

Regarding the system of iF3H20/C14OH, at  $X(\text{C14OH}) = 0.2$ , dark domains on a gray background are visible. Since the collapse pressure is characteristic for iF3H20, it seems that the system contains a homogeneous monolayer of iF3H20 and separated domains of a C14OH monolayer. At  $X(\text{C14OH}) = 0.5$  (Figure 6b), gray domains of C14OH grow in size and fuse and new circular white spots appear. This new phase can be ascribed to 3D crystallites of iF3H20, since the collapse pressure is characteristic of this substance for each mixed film composition. For  $X(\text{C14OH}) = 0.8$ , the image is slightly different because two kinds of circular domains can be observed. Some are larger and gray while others are smaller and white. It seems that the larger gray domains contain alcohol in a liquid expanded state, whereas the white smaller domains correspond to 3D crystallites of iF3H20. Regarding the iF3H20/C22OH system, at  $X(\text{C22OH}) = 0.2$ , the film is homogeneous which proves the presence of complete mixing between the components. At  $X(\text{C22OH}) = 0.5$ , some white spots are observed, which can be interpreted as the appearance of some nuclei of a crystalline iF3H20 phase on the mixed monolayer surface. At this concentration, the  $\pi_C$  is much greater than the value character-

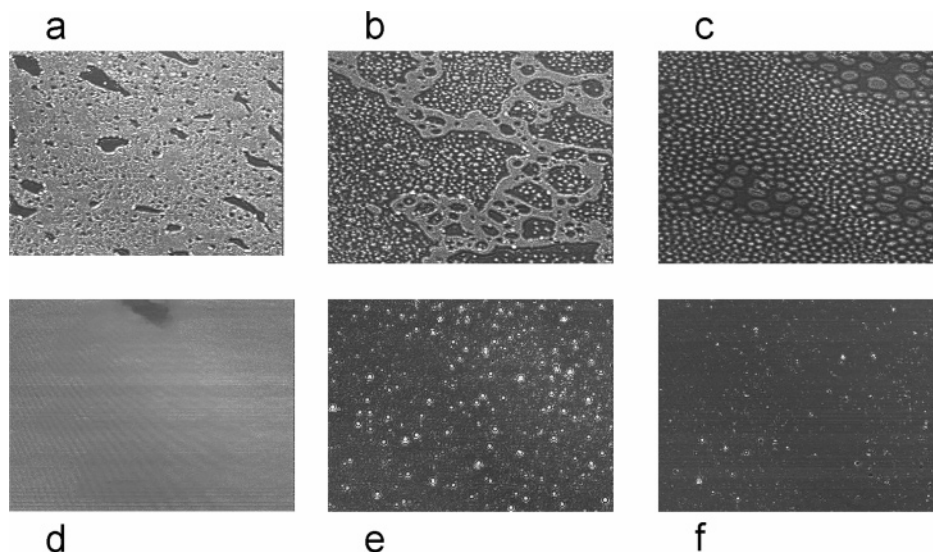


**Figure 6.** BAM images for mixtures of iF3H20 with alcohols, registered at 5 mN/m: (a–c) iF3H20/C14OH (a)  $X(\text{C14OH}) = 0.2$ , (b)  $X(\text{C14OH}) = 0.5$ , (c)  $X(\text{C14OH}) = 0.8$ ; (d–f) iF3H20/C22OH (d)  $X(\text{C22OH}) = 0.2$ , (e)  $X(\text{C22OH}) = 0.5$ , (f)  $X(\text{C22OH}) = 0.8$ .

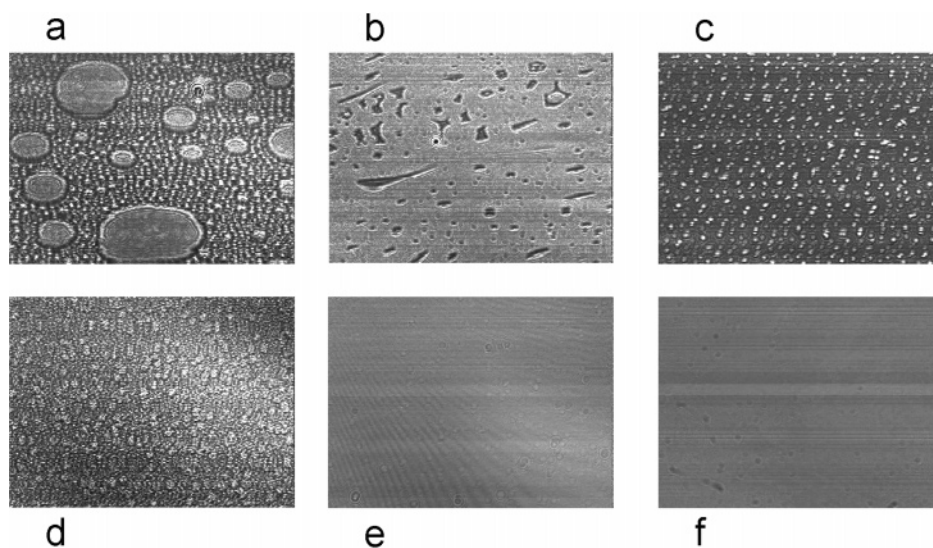


**Figure 7.** BAM images for mixtures of F4H20 with C14OH and C22OH, registered at 5 mN/m: (a–c) F4H20/C14OH (a)  $X(\text{C14OH}) = 0.2$ , (b)  $X(\text{C14OH}) = 0.5$ , (c)  $X(\text{C14OH}) = 0.8$ ; (d–f) F4H20/C22OH (d)  $X(\text{C22OH}) = 0.2$ , (e)  $X(\text{C22OH}) = 0.5$ , (f)  $X(\text{C22OH}) = 0.8$ .

istic for a pure iF3H20 monolayer, while at  $X(\text{C22OH}) = 0.8$  the number of white spots is very small, indicating a better miscibility as compared to a 1:1 mixture ( $X = 0.5$ ). Generally, there is a good agreement between BAM images and  $\pi_C$ – $X(\text{C22OH})$  plots for this system.

Figure 7a–c shows images registered for the system F4H20/C14OH. In Figure 7a, gray domains are present, which can be ascribed to C14OH monolayer domains, as the  $\pi_C$  is characteristic for F4H20. In Figure 7b, dark irregular domains on a gray background are seen and, since the  $\pi_C$  value is characteristic of a F4H20 monolayer, can be interpreted as separated domains of a C14OH monolayer. On the contrary, white spots in Figure 7c can be described as nuclei of a F4H20 3D phase on the C14OH monolayer, as the  $\pi_C$  at this mole fraction is characteristic of the investigated alcohol. Different data were obtained for the system F4H20/C22OH. In the case of  $X(\text{C22OH}) = 0.2$ , a large number of small circular domains is visible, which can indicate phase separation. For  $X(\text{C22OH})$  greater than 0.3, the monolayers were homogeneous until  $\pi_C$  and no structures were observed. The data obtained from BAM experiments are in accordance with the  $\pi_C$ – $X(\text{alcohol})$  dependencies.

### 3.2 Mixed Monolayers Formed by SFAs with a Long Perfluorinated Moiety.

In a similar set of experiments to those described above, four systems of mixed monolayers, namely, iF9H20/C14OH, iF9H20/C22OH, F10H20/C14OH, and F10H20/C22OH, were investigated. Both SFAs selected for this part of our research have a long perfluorinated moiety, one in normal constitution (F10H20) and one with an *iso*-branching (iF9H20). The experiments were carried out following the same procedure as in the case of SFAs with a short perfluorinated fragment. Figure 8 shows  $\pi$ – $A$  isotherms for the four systems of mixed monolayers. In all four systems, the addition of alcohol to the SFA monolayer has a condensing effect, which means that with the increasing mole fraction of alcohol the  $\pi$ – $A$  isotherm shifts toward smaller molecular areas.

Compression moduli values were also calculated for all four systems discussed here, which enabled the unambiguous determination of collapse pressures of the mixed systems. Figure 9 presents collapse pressures– $X(\text{alcohol})$  dependencies for the four studied systems. Generally, for mole fractions of alcohol up to 0.4, an increase of  $\pi_{\text{coll}}$  is observed; for  $X(\text{alcohol}) = 0.5$  and 0.6, it is rather difficult to determine precisely what the  $\pi_{\text{coll}}$  value is, while for  $X(\text{alcohol}) = 0.7$  and greater  $\pi_{\text{coll}}$  values,



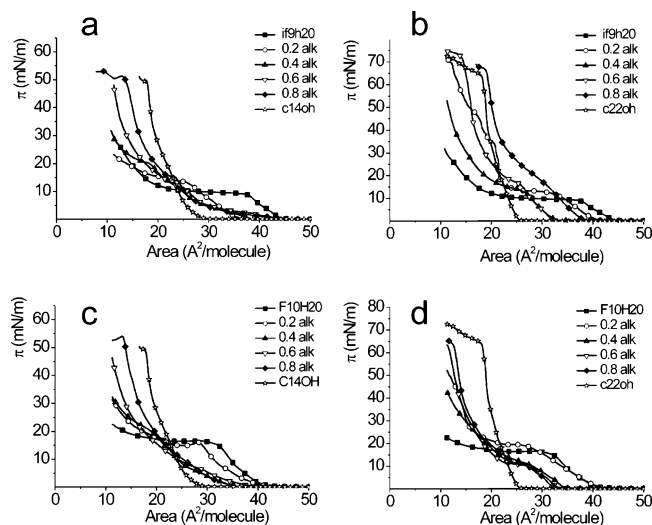


**Figure 8.** Plots of  $\pi$ - $A$  isotherms for the mixed monolayers formed by iF9H20 and F10H20: (a) iF9H20/C14OH; (b) iF9H20/C22OH; (c) F10H20/C14OH; (d) F10H20/C22OH.

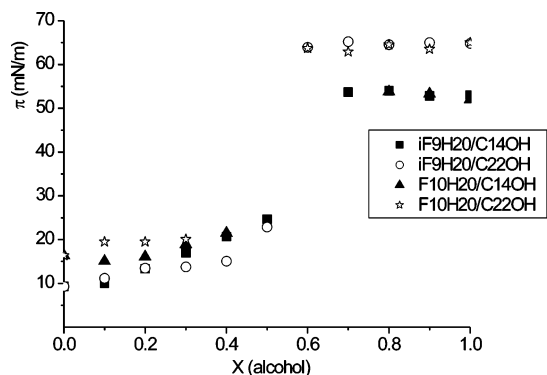


**Figure 9.** Collapse pressures ( $\pi_c$ ) vs alcohol mole fraction ( $X$ ) for the systems containing iF9H20 and F10H20.

typical for alcohol monolayers, were registered. The increase of  $\pi_{coll}$  with rising  $X(\text{alcohol})$  can indicate that a 2D mixture is formed and that phase separation does not take place.

On the basis of the  $\pi$ - $A$  dependencies for the mixed monolayers, interaction parameter  $\alpha$  values were calculated for selected surface pressures (lower than  $\pi_c$  of a pure SFA monolayers) and the plots  $\alpha$  vs the mole fraction of a given alcohol are presented in Figure 10. The most noticeable feature of these plots is the change of the sign in the  $\alpha$ - $X(\text{alcohol})$  dependencies. For lower mole fractions of alcohols up to 0.6, the  $\alpha$  values are negative or close to zero, while for greater alcohol proportions they are positive. The change of the sign of the  $\alpha$ - $X(\text{alcohol})$  dependencies indicates that for some mole fractions of a given alcohol the interaction between the alcohol and SFA molecules is more attractive than between the molecules in a pure alcohol or a SFA monolayer, whereas a positive sign of  $\alpha$  for greater mole fractions of alcohol means that the interaction between the alcohol and SFA molecules is less attractive or even repulsive; therefore, a hypothesis can be proposed that, for mixed film compositions containing alcohol in excess, phase separation in the mixed monolayers can occur.

Together with mechanic and thermodynamic characterization of the mixed monolayer, BAM observations were performed and the representative BAM images are gathered in Figure 11. Images 11 a-c show the structures of mixed monolayers for the system: iF9H20/C14OH, registered at  $\pi = 5$  mN/m, for  $X(\text{C14OH}) = 0.2$  (11a), 0.5 (11b), and 0.8 (11c). The value of 5 mN/m was chosen because it lies approximately in the middle

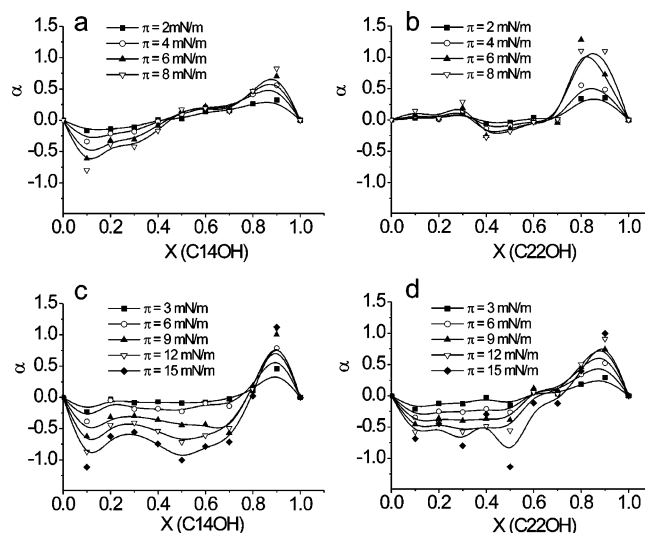


**Figure 10.** Interaction parameters ( $\alpha$ ) vs alcohol mole fraction ( $X$ ) for the systems containing iF9H20 and F10H20.

between the surface pressure *set-off* and the monolayer collapse pressure for a pure iF9H20 monolayer. A great number of white small domains in Figure 11a indicates that, at a large proportion of iF9H20, C14OH forms small domains and does not mix with the SFA film. Figure 11b shows a practically homogeneous mixed monolayer without any visible structures, while in Figure 10c gray, circular structures can be observed and, because of the high value of  $\pi_c$ , they are interpreted as iF9H20 3D crystallites. In the case of iF9H20/C22OH, mixed monolayers are homogeneous up to the collapse pressure, regardless the mole ratio of C22OH, and because of this fact, their BAM images are not presented here. Some representative BAM images for the system F10H20/C14OH are shown in Figure 11d-f. The images were taken at  $\pi = 5$  mN/m and  $X(\text{C14OH}) = 0.2$  (11d), 0.5 (11e), and 0.8 (11f). In Figure 11d, only a few white spots are visible, which can be interpreted to indicate that the mixed monolayer is generally homogeneous and only a small amount of C14OH forms separate domains. Figure 11e and f shows images of phase separated systems. In the fourth system F10H20/C22OH, only homogeneous monolayers are observed, and no nucleation proceeds until the collapse.

#### 4. Discussion

On the basis of BAM images,  $\pi$ - $A$  isotherms, compression moduli, and  $\pi_{coll}$ - $X(\text{alcohol})$  dependencies, it was possible to draw phase diagrams for all 8 systems of mixed monolayers described in this contribution. Roman numerals used in the phase diagrams indicate the number of phases present at a given surface pressure and alcohol mole fraction. Figure 12 shows phase diagrams for the investigated four systems containing tetradecanol. It is visible that the phase behavior of these systems depends on the structure of a semifluorinated alkane. All the SFAs investigated here have the same length of the hydrogenated chain (20 carbon atoms), so the key difference seems to be hidden in the structure and dimension of the perfluorinated moiety.

The components of the system iF3H20/C14OH (Figure 12a) are immiscible in the whole range of mole fractions. At surface pressures lower than the value of the collapse pressure for a pure iF3H20 monolayer (ca. 8 mN/m) and the mole fraction of C14OH lower than 0.5, two phases are present: separated domains of iF3H20 and C14OH monolayers. At a larger alcohol proportion, crystallites of iF3H20 appear even at surface pressure

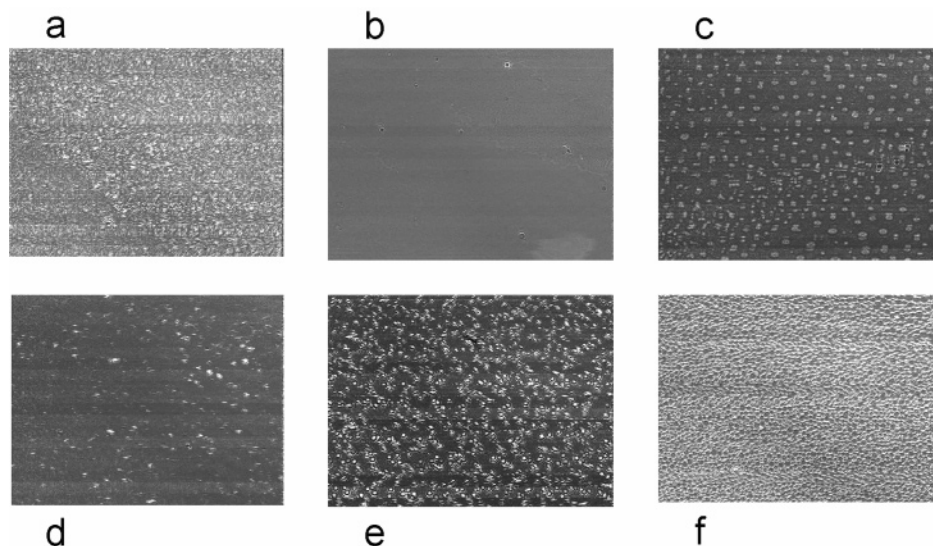


**Figure 11.** BAM images for mixtures of iF9H20 and F10H20 with C14OH, registered at 5 mN/m: (a–c) iF9H20/C14OH (a)  $X(\text{C14OH}) = 0.2$ , (b)  $X(\text{C14OH}) = 0.5$ , (c)  $X(\text{C14OH}) = 0.8$ ; (d–f) F10H20/C14OH (d)  $X(\text{C14OH}) = 0.2$ , (e)  $X(\text{C14OH}) = 0.5$ , (f)  $X(\text{C14OH}) = 0.8$ .

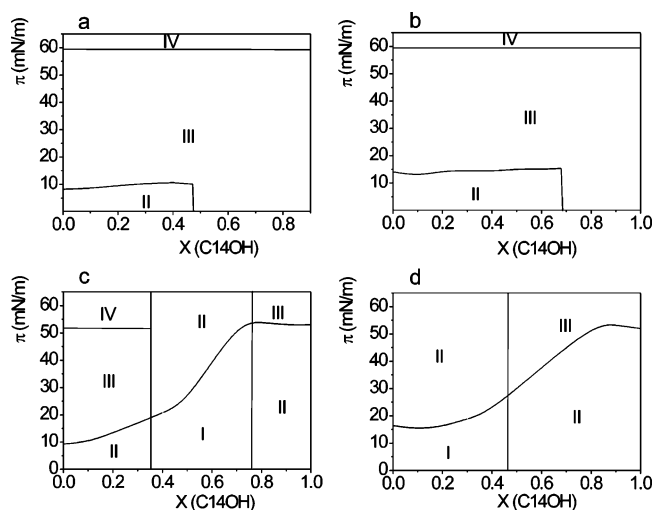


**Figure 12.** Phase diagrams for the systems containing iF3H20 and F4H20.

values close to 0 and the system contains 3 phases: domains of C14OH monolayer and crystallites of iF3H20, which are in equilibrium with an iF3H20 monolayer. At  $\pi$  values close to 60 mN/m, a fourth phase—multilayer domains of C14OH—appears. The system F4H20/C14OH (Figure 12b) is very similar to the former one, only the range of 2 phase coexistence is wider (up to  $X(\text{C14OH}) \approx 0.7$ ).

The phase situation in the systems containing tetradecanol and SFAs with a longer perfluorinated moiety is pronouncedly different. The phase diagram of iF9H20/C14OH (Figure 12c) is the most complicated. At  $X(\text{C14OH})$  lower than 0.4, the system is immiscible, and below the collapse pressure of iF9H20, two phases are present: a monolayer of iF9H20 and separate domains of C14OH monolayer. Upon ca. 8 mN/m, three phases can be distinguished: domains of a C14OH monolayer and crystallites of SFA which are in equilibrium with its monolayer. Meanwhile, at high values of  $\pi$ , ca. 60 mN/m, a fourth phase occurs—multilayer domains of C14OH. At  $X(\text{C14OH})$  ranging from 0.4 to ca. 0.8, the system is miscible, whereas, at a high proportion of C14OH, iF9H20 crystallites separate from the mixed monolayer and two phases are present: 2- and 3-dimensional phases. In the case of the system F10H20/C14OH (Figure 12d), the phase situation is partially different. At

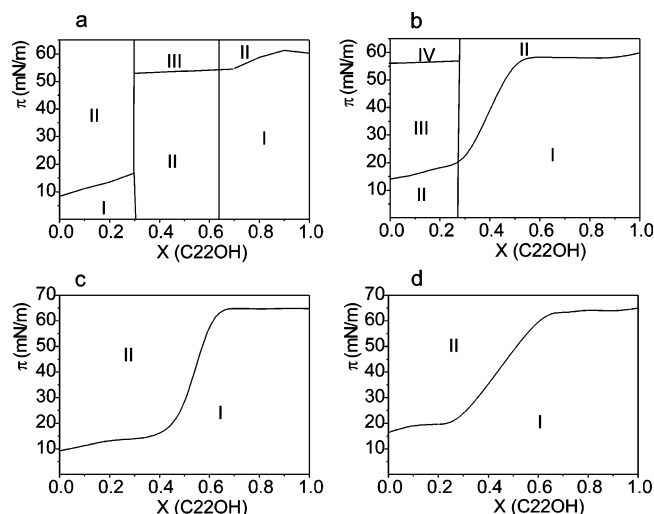


**Figure 13.** Phase diagrams of the systems containing iF9H20 and F10H20.

$X(\text{C14OH})$  ranging from 0 to ca. 0.5, the two substances are miscible and a homogeneous monolayer was observed below the collapse pressure, whereas at higher mole fractions of the alcohols crystallites of F10H20 were present from the beginning of the rise in surface pressure.

Figure 13 presents phase diagrams for the four systems containing docosanol. The system iF3H20/C22OH (Figure 13a) is miscible at low docosanol concentrations (below  $X(\text{C22OH}) = 0.3$ ) and at high alcohol concentrations ( $X(\text{C22OH})$  greater than 0.6), whereas at comparable mole fractions of the components the system is immiscible and 3D crystallites were visible in BAM images even at low surface pressures. So at these compositions, the system contains two phases: iF3H20 crystallites in equilibrium with the mixed monolayer. At a high value of surface pressure (greater than 50 mN/m), a third phase occurs: a multilayer of C22OH. The system F4H20/C22OH (Figure 13b) is immiscible at low concentrations of docosanol ( $X(\text{C22OH})$  lower than ca. 0.3), whereas for greater alcohol concentrations the system is miscible. In the case of semifluorinated alkanes with a long perfluorinated moiety (Figure 13c and d), regardless of its constitution (with or without *iso*-branching), homogeneous single-phase mixed monolayers were formed for all molar fractions of C22OH.



On the basis of the results obtained in this paper, it is possible to draw some conclusions concerning the mixing behavior of semifluorinated alkanes and alcohols. Generally, all four SFAs chosen for our investigation mix much better with docosanol than with tetradecanol. As it has already been pointed out, semifluorinated alkanes do not possess any hydrophilic group and at the water/air interface are oriented with their perfluorinated part toward the air phase. The formation of monomolecular films of semifluorinated alkanes at the free surface of water is possible due to the van der Waals interactions between SFA molecules at the interface.<sup>45</sup> As far as the interactions between a SFA and an alcohol molecule in a mixed film are concerned, the van der Waals forces can also be treated as a crucial factor for determining their mutual interaction and miscibility, for SFA molecules do not possess any hydrophilic or ionizable group and are not charged. These van der Waals forces are additive<sup>46</sup> and can be treated as a sum of contributions from atoms and groups of atoms. In our case, the building blocks are CH<sub>2</sub> and CF<sub>2</sub> groups. The interactions between CH<sub>2</sub> groups from different chains are attractive. All the SFAs investigated here have the same length of the hydrogenated moiety, containing 20 carbon atoms or 19 methylene and one methyl groups, so it is easy to predict that the interaction with an alcohol molecule with a longer chain will be more attractive and stronger than with an alcohol molecule with a shorter chain. Another influencing factor is the length of the perfluorinated moiety; two CF<sub>2</sub> groups from different chains also attract each other, so generally, monolayers formed by a SFA with a longer perfluorinated moiety should be better organized and more condensed than those formed by a SFA with a short perfluorinated fragment, which was confirmed in our previous paper.<sup>32</sup> Generally, it seems that mixtures containing SFAs with a long perfluorinated moiety and alcohols with a longer hydrogenated chain should be more condensed as compared to mixed films containing SFAs with a short perfluorinated fragment and alcohols with a shorter hydrogenated chain. Such a tendency was corroborated by this research, because all four SFAs selected for our investigation have a broader range of mutual miscibility with C22OH than with C14OH; moreover, SFAs with a long perfluorinated chain mix to a larger extent with both alcohols than SFAs with a short perfluorinated group. Another factor that is important here can be the behavior of alcohol molecules in pure alcohol films at the water/air interface. Alcohols with the number of carbon atoms larger than 15 form at room temperature very condensed monolayers, while alcohols with shorter hydrocarbon chains form more expanded films.<sup>1</sup> Branching of the perfluorinated chain can also play here an important role, as the additional CF<sub>3</sub> group at the terminal position can be considered to be a steric hindrance, which results in less-condensed monolayers of *iso*-branched SFAs as compared to the films formed by their analogues with normal chain constitution.

We think that, in future investigations of more complicated systems, signaled in the Introduction, the use of perfluorodecyl eicosane F10H20 and natural surfactants containing more than 14 carbon atoms in their hydrocarbon chain is advisable. The choice of F10H20 results from the fact that it forms very stable monolayers of a considerably high collapse pressure (ca. 16 mN/m) as compared to the other semifluorinated alkanes investigated here. Moreover, the perfluorodecyl iodide required for the synthesis of F10H20 is commercially available and is of reasonable purity and price.

The results of our investigations shed light on the interaction between semifluorinated alkanes and model surfactants with

small headgroups, namely, long-chain fatty alcohols. It was shown that the simplicity of the structure of surfactants used in researching mixed Langmuir monolayers does not necessarily lead to simplicity in phase behavior. The interactions between SFAs and the hydrogenated alcohols depend on many factors; however, some general trends can be noticed. Studies of interactions between perfluorinated, semifluorinated, and hydrogenated chains are important in the design of a new generation of drugs and allow a better understanding of the behavior of model systems, which can be of much help in designing mixed systems involving molecules of more complicated architectures.

## References and Notes

- (1) Gaines, G. L., Jr. *Insoluble Monolayers at the Liquid-Gas Interfaces*; Wiley Interscience: New York, 1966.
- (2) Durand, D. J.; Clyman, R. I.; Hyman, M. A.; Clements, J. A.; Mauray, F.; Kittermann, J.; Ballard, P. *J. Pediatr.* **1985**, *109*, 775.
- (3) Lawrie, G. A.; Gentle, J. R.; Barnes, G. T. *Colloids Surf., A* **2001**, *171*, 217.
- (4) Chen, K. B.; Chang, C. H.; Yang, Y. M.; Maa, J. R. *Colloids Surf., A* **2000**, *170*, 199.
- (5) Takao, Y.; Yamauchi, H.; Manosroi, J.; Manosroi, A.; Abe, M. *Langmuir* **1995**, *11*, 912.
- (6) Dynarowicz-Lątka, P.; Hąc-Wydro, K. *Colloids Surf., B* **2004**, *37*, 21.
- (7) Ries, H. E., Jr.; Swift, H. S. *J. Colloid Interface Sci.* **1978**, *64*, 111.
- (8) Abriouel, H.; Sanchez-Gonzalez, J.; Maqueda, M.; Galvez, A.; Valdivia, E.; Galvez-Ruiz, M. J. *J. Colloid Interface Sci.* **2001**, *233*, 306.
- (9) Dynarowicz-Lątka, P.; Ramon Seoane, J.; Miñones-Trillo, J.; Conde Mouzo, O.; Casas Parada, M. *Bull. Pol. Acad. Sci., Chem.* **1999**, *47*, 153.
- (10) Vila-Romeu, N.; Nieto-Suarez, M.; Dynarowicz-Lątka, P.; Prieto, I. *J. Phys. Chem. B* **2002**, *106*, 9820.
- (11) Sparr, E.; Eriksson, L.; Bouwstra, J. A.; Ekelund K. *Langmuir* **2001**, *17*, 164.
- (12) Lee, Y. J.; Rho, H. S.; Kim, D. H.; Kim, J. D. *Colloids Surf., A* **2002**, *205*, 173.
- (13) Capuzzi, G.; Kulkarni, K.; Fernandez, J. E.; Vincieri, F. F.; Lo Nostro, P. *J. Colloid Interface Sci.* **1997**, *186*, 271.
- (14) Rey Gomez-Serranillos, I.; Miñones, J., Jr.; Dynarowicz-Lątka, P.; Iribarnegaray, E.; Casas, M. *Colloids Surf., B* **2005**, *41*, 63.
- (15) Roy Gomez-Serranillos, I.; Miñones, J., Jr.; Dynarowicz-Lątka, P.; Miñones, J.; Conde, O. *Langmuir* **2004**, *20*, 11414.
- (16) Krafft, M. P.; Riess, J. G. *Biochimie* **1998**, *80*, 489.
- (17) Riess, J. G. *Tetrahedron* **2002**, *58*, 4113.
- (18) Scott, R. L. *J. Am. Chem. Soc.* **1948**, *70*, 4090.
- (19) Hildebrand, J. H. *J. Am. Chem. Soc.* **1950**, *72*, 4348.
- (20) Mukerjee, P.; Yang, A. Y. S. *J. Phys. Chem.* **1976**, *80*, 1388.
- (21) Mukerjee, P. *Colloids Surf., A* **1994**, *84*, 1.
- (22) Nakahara, H.; Nakamura, S.; Kawasaki, H.; Shibata, O. *Colloids Surf., B* **2005**, *41*, 67.
- (23) Arora, M.; Bummer, P. M.; Lehmler, H. J. *Langmuir* **2003**, *19*, 8843.
- (24) Lehmler, H. J.; Jay, M.; Bummer, P. M. *Langmuir* **2000**, *16*, 10161.
- (25) Imae, T.; Takeshita, T.; Kato, M. *Langmuir* **2000**, *16*, 612.
- (26) Shibata, O.; Krafft, M. P. *Langmuir* **2000**, *16*, 10281.
- (27) Courier, H. M.; Vandamme, T. F.; Krafft, M. P.; Nakamura, S.; Shibata, O. *Colloids Surf., A* **2003**, *215*, 33.
- (28) Shibata, O.; Yamamoto, S. K.; Lee, S.; Sugihara, G. *J. Colloid Interface Sci.* **1996**, *184*, 201.
- (29) Turberg, M. P.; Brady, J. E. *J. Am. Chem. Soc.* **1988**, *110*, 7797.
- (30) Gaines, G. L., Jr. *Langmuir* **1991**, *7*, 3054.
- (31) Huang, Z.; Acero, A. A.; Lei, N.; Rice, S. A.; Zhang, Z.; Schlossman, M. I. *J. Chem. Soc., Faraday Trans.* **1996**, *92*, 545.
- (32) Broniatowski, M.; Sandez Macho, I.; Miñones, J., Jr.; Dynarowicz-Lątka, P. *J. Phys. Chem. B* **2004**, *108*, 13403.
- (33) Broniatowski, M.; Dynarowicz-Lątka, P. *J. Fluorine Chem.* **2004**, *125*, 1501.
- (34) Krafft, M. P.; Giulieri, F.; Fontaine, P.; Goldmann, M. *Langmuir* **2001**, *17*, 6577.
- (35) Maaloum, M.; Muller, P.; Krafft, M. P. *Langmuir* **2004**, *20*, 2261.
- (36) Wang, S.; Lunn, R.; Krafft, M. P.; Leblanc, R. M. *Langmuir* **2000**, *16*, 2882.
- (37) Simoes Gamboa, A. L.; Filipe, E. J. M.; Brogueira, P. *Nano Lett.* **2002**, *2*, 1083.

- (38) Rabolt, J. F.; Russell, T. P.; Twieg, R. J. *Macromolecules* **1984**, *17*, 2786.
- (39) Ries, H. E.; Kinball, W. A. *J. Phys. Chem.* **1955**, *59*, 91.
- (40) Lu, W.; Knobler, C. M.; Bruinsma, R. F.; Twardos, M.; Dennim, M. *Phys. Rev. Lett.* **2002**, *89*, 146107.
- (41) Nikomarov, E. S. *Langmuir* **1990**, *6*, 999.
- (42) Harkins, W. D., *The Physical Chemistry of Surface Films*; Reinhold Publishing Co.: New York, 1954; p 107.
- (43) Davies, J. T.; Rideal, E. K., *Interfacial Phenomena*, 2nd ed.; Academic Press: New York, 1963; pp 265 and 65.
- (44) Dynarowicz-Łątka, P.; Kita, K. *Adv. Colloid Interface Sci.* **1999**, *79*, 1.
- (45) Li, M.; Acero, A. A.; Huang, Z.; Rice, S. A. *Nature* **1994**, *367*, 151.
- (46) Israelachvili, J. N. *Intermolecular and Surface Forces*; Academic Press: New York, 1995.